physica status solidi

pss

www.pss-journals.com

reprint

WILEY-VCH

Phys. Status Solidi C **11**, No. 11–12, 1634–1639 (2014) / **DOI** 10.1002/pssc.201431562

physica status solidi c
www.pss-c.com
current topics in solid state physics

Oxygen gettering in low-energy arsenic or antimony ion implanted Cz-silicon

O. Oberemok[1], V. Kladko[1], V. Litovchenko[*,1], B. Romanyuk[1], V. Popov[1], V. Melnik[1], and J. Vanhellemont[,2]**

[1] V. Lashkarev Institute of Semiconductor Physics, NAS of Ukraine, Prospect Nauki 41, 03028 Kyiv, Ukraine
[2] Department of Solid State Sciences, Ghent University, Krijgslaan 281 S1, 9000 Ghent, Belgium

Received 28 March 2014, revised 7 August 2014, accepted 15 August 2014
Published online 19 September 2014

Keywords ion implantation, Si p-n junction, annealing, depth profile, oxygen, arsenic, antimony, gettering

* Corresponding author: e-mail lvg@isp.kiev.ua, Phone: +38-044-5256290, Fax: +38-044-5256290;
** e-mail jan.vanhellemont@ugent.be, Phone: +32-499-593857, Fax: +32-9-2644996

Low energy As or Sb ion implantation followed by furnace annealing was used to create ultra shallow junctions. It was found that a significant amount of oxygen was redistributed from the Si bulk to the As implanted layer leading even to an increase of the screening oxide film thickness. Using a marker layer created by implantation of ^{18}O ions, it was confirmed that a large number of interstitial oxygen atoms are transferred from the bulk of the Si wafer to the wafer surface during implanted As activation annealing. Estimation of the O diffusivity in Si during the 950 °C activation anneal, yields a value of about 10^{-10} cm^2/s which is more than an order of magnitude larger than the literature value which is close to 7×10^{-12} cm^2/s. In the case of Sb implantation, the oxygen gettering effect is much reduced. This difference in oxygen behavior can be attributed to the influence of mechanical stress in the near surface highly doped layer. The configuration of the mechanical stress field is different for the cases of As and Sb implantation, with tensile stress dominating for the latter.

1 Introduction The formation of low resistive shallow junctions is one of the major challenges for the further scaling down of metal-oxide-semiconductor field-effect transistors (MOSFET's) dimensions. As the gate length decreases, the depth of source and drain areas has to be reduced to suppress short channel effects. The fabrication of sub 100 nm MOSFETs, using low-energy ion implantation, has been reported already several years ago [1].

In particular, low energy implantation of As or Sb ions is widely used to create ultra shallow n^+-p junctions (USJ's). However, the formation of a high quality USJ is complicated by dopant deactivation, dopant accumulation near the SiO_2-Si interface [2], and also by transient enhanced diffusion (TED) as a result of the interaction of dopant atoms with intrinsic point defects created by the implantation [3].

Dopant-intrinsic point defect interactions under strongly non equilibrium intrinsic point defect concentrations, dopant diffusion for very high dopant concentrations, and dopant deactivation processes due to precipitation or formation of dopant-intrinsic point defect complexes should be understood quantitatively and accurately simulated in order to control UJS formation.

Another important factor affecting the properties of USJ's in Czochralski-grown Si is the presence of interstitial oxygen with a concentration of the order of 10^{18} cm^{-3}. It is well-known that oxygen precipitation in Si leads to formation of defects that act as gettering centers for metal impurities that can be responsible for increased leakage current [4,5]. Oxygen is also rapidly gettered into residual damage regions, forming stable SiO_x precipitates during annealing [6]. It was previously shown that high-energy implanted As ions can influence the stoichiometry of the screening oxide [7]. A local increase of the oxygen concentration above 10^{20}cm^{-3} in the heavily As doped shallow junction layer, can lead to degradation of electrical characteristics and reduction of the carrier mobility [8]. The reason for this behavior is the formation of electrically in-

active As-O [9] or O-As-Vacancy clusters [10]. All of the effects above can lead to a degradation of the devices.

In a previous study [11] oxygen redistribution in As implanted Si wafers was studied, revealing oxygen gettering in the heavily As doped subsurface layer during thermal annealing, as well as a measurable increase of the screen oxide thickness.

In the present study, USJ's were created by low-energy As^+ or Sb^+ implantation followed by dopant activation furnace annealing. The redistribution of As, Sb and O atoms during the annealing was studied using Secondary Ion Mass Spectrometry (SIMS). A buried oxygen marker layer created by ^{18}O isotope implantation, was used for measuring the oxygen diffusion towards the As or Sb implanted region. Oxygen gettering and defect generation mechanisms for As or Sb ion implantation were compared.

2 Experimental All the experiments were performed on (100), 10 Ωcm, p-type Cz-silicon wafers containing about 10^{18} cm^{-3} interstitial oxygen atoms. The samples were implanted through a 2.2 nm screening oxide with 4×10^{14} cm^{-2}, 5 keV As^+ or Sb^+ ions. Some of the samples were additionally ion implanted with $^{18}O^+$ (100 keV, 1.2×10^{14} cm^{-2}).

Furnace annealing of the as-implanted samples was carried out in nitrogen ambient for 0.5 to 20 minutes using temperatures between 750 °C and 950 °C. The average heating and cooling rates were 25 °C and 30 °C per second, respectively.

Analysis of the dopant depth profiles was performed by SIMS using Cameca IMS 4F and ToF-SIMS IV instruments. The depth scale was determined for each profile by measuring the crater depth with a Dektak 3030 profilometer.

Lattice defect creation and transformation were investigated by X-ray diffuse scattering (XDS) using a high-resolution diffractometer PANalytical X'Pert Pro MRD.

3 Observations

3.1 SIMS results SIMS depth profiles of As and Sb dopants and the $^{60}SiO_2^-$ signal depth distribution before and after annealing at 950 °C for 1, 5 and 20 minutes are shown in Fig. 1. It can be seen that after annealing, the implanted As is redistributed both towards the surface and towards the bulk of the sample. Arsenic accumulation at the SiO_2-Si interface is increasing with annealing temperature and duration. It was also observed that the As redistribution is accompanied by changes in the oxygen concentration ($^{60}SiO_2^-$ intensity) in the vicinity of the USJ. In the following we call this region the Active Diffusion Region (ADR) of impurities that is located between 3 (at the SiO_2-Si interface) and 100 nm below the wafer surface.

An increase of the SiO_2^- signal by a factor of 3 is observed after an anneal at 950 °C for 1 minute compared to as-implanted sample, clearly illustrating that the concentration of oxygen in the ADR increases during thermal annealing.

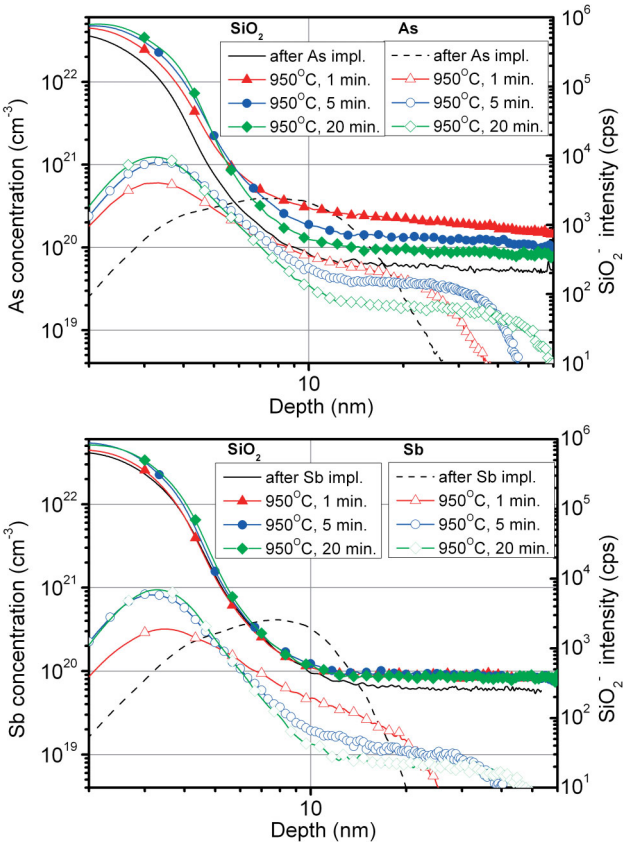

Figure 1 SIMS depth profiles of As (top), Sb (bottom) and $^{60}SiO_2^-$ distributions after annealing at 950 °C for 1, 5 and 20 min.

Annealing of the As implanted samples leads to an increase of the screening silicon oxide layer thickness and to a recovery of the surface film to the SiO_2 composition. In a previous study [11], it was shown that this effect is the result of oxygen gettering to the ADR from the bulk of the Si wafer followed by oxygen segregation at the SiO_2/Si interface.

Estimation of the oxide thickness at the 0.707 level from the maximum of the initial oxygen depth profile shows that the increase of annealing temperature leads to an increase in the screening oxide film thickness from 2.2 to 2.8 nm. The maximum oxygen concentration in the ADR is reached after 1 and 3 min annealing at 950 °C and 750 °C, respectively.

The oxygen gettering process in the ADR happens mainly during the initial stage of thermal annealing. After that, the process of the surface oxide film growth due to absorption of oxygen from the ADR begins. In the same time interval, the processes of implanted As redistribution and activation [2,3] take place suggesting that the O and As redistribution are correlated.

At an anneal temperature of 750 °C, a significant As redistribution towards the surface occurs only after 5 min annealing and As accumulation at the SiO_2-Si interface only for anneals longer than 20 min. At 950 °C, a substantial As accumulation at the interface begins already after 0.5 min annealing.

The shallow junction creation by Sb implantation does not lead to an increase of the surface oxide thickness (Fig. 1) for all the temperatures and times of activation annealing. Only a small increase of oxygen concentration in the ADR is observed after annealing at 900 or 950 °C, but at lower temperatures no changes in oxygen distribution were not detected.

It should also be noted that at 750 or 800 °C, Sb segregation proceeds much slower than in the case of As. After annealing at 750 °C for 5 to 20 minutes, more than half of the implanted As atoms are segregated at the SiO_2 surface layer. For the same conditions, the number of Sb atoms which are segregated at the SiO_2/Si interface is much smaller [3, 11] and the SiO_2 layer thickness remains unchanged.

3.2 XDS results A significant difference is observed between the XDS spectra for As and Sb implanted samples after annealing. After implantation of As^+ or Sb^+ ions, both vacancy and interstitial defects are observed as illustrated in Fig. 2.

The XDS observations indicate the existence of high mechanical stresses in the implanted region [12]. The shapes of the recorded curves indicate that all the samples contain defects both of vacancy ($\mathbf{q}_z < 0$), and of interstitial ($\mathbf{q}_z > 0$) type, where $\mathbf{q}_z$ is the reciprocal lattice vector.

For the As implanted samples, the concentration of both types of defects increases after annealing at 750 °C. After annealing at 950 °C, the vacancy defects almost disappear, while at the same time the concentration of interstitial defects increases.

In the Sb implanted samples, there is accumulation of vacancy-type defects and an almost complete absence of interstitial defects during annealing at 750 °C. The annealing time does not affect the concentration of these defects. Increasing the annealing temperature to 950 °C, leads to a decrease in the concentration of vacancy defects, but their concentration is still much higher than in the samples implanted by As. Extending the annealing time at 950 °C leads to a slight increase of the concentration of interstitial defects.

In single crystal Si with lattice parameter a, As implantation leads to both tensile ($^{\Delta a}/_a = 7.7 \times 10^{-4}$) and compressive ($^{\Delta a}/_a = -5.64 \times 10^{-4}$) strained regions. The tensile deformation in the Sb implanted samples is higher ($^{\Delta a}/_a = -1.03 \times 10^{-3}$) than in the As implanted ones, in agreement with the larger atom size. No compressive strained regions are observed after Sb implantation.

In the Sb implanted samples there exist only tensile mechanical stresses. Therefore, there is also no stress gradient, and oxygen gettering does not take place.

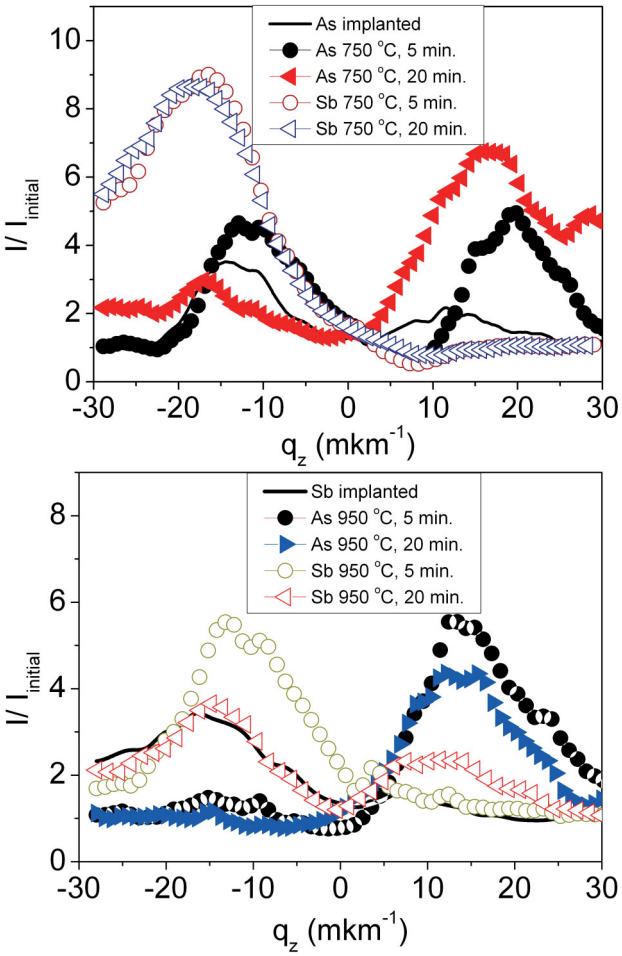

Figure 2 XDS curves for As and Sb implanted Si (solid curves) and after annealing at 750 °C (top) and 950 °C (bottom).

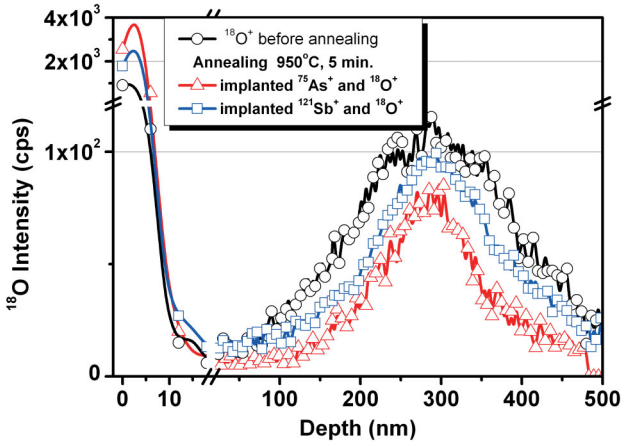

Figure 3 SIMS ^{18}O depth profiles for samples co-implanted by $^{75}As^+$ or $^{121}Sb^+$ and $^{18}O^+$ before and after annealing at 950 °C for 5 min.

3.3 Behavior of the ^{18}O marker layer during annealing One can assume that the bulk of the Si wafer is the main source of oxygen to explain the observed oxide layer growth in the case of As implantation. To confirm this assumption, an ^{18}O marker layer was introduced at a depth of 0.3 μm from the sample surface by ion implantation. This buried layer will act as an oxygen source during the annealing and activation of the implanted As^+ ions. It is necessary to use ^{18}O isotope to be able to separate the implanted oxygen from the background ^{16}O oxygen that is always present in Cz Si.

Figure 3 shows concentration depth profiles of the implanted ^{18}O marker atoms determined by SIMS before and after annealing at 950 °C for 5 minutes of As or Sb implanted samples. The projected range of oxygen was close to 300 nm. It is seen that the implanted ^{18}O is much more redistributed towards the As implanted region and is incorporated also into the screen oxide layer on the wafer surface. In the presence of the ^{18}O marker layer, the thickness of the screen oxide layer is increased by about 0.5 nm after annealing. For the Sb^+ implanted samples, the oxygen redistribution towards the surface is much smaller.

4 Discussion

4.1 Dopant and oxygen redistribution At the beginning of the 750 °C anneal, reconstruction of the implanted region defect structures occurs and simultaneously oxygen gettering from the wafer bulk takes place in the As implanted samples. The driving force for oxygen gettering in the ADR is the tensile mechanical stress gradient in the near surface region with the highest As concentration.

For anneals at 750 °C longer than 20 min, only a fraction of the As atoms is located in substitutional lattice sites, while the rest of the As atoms is accumulated at the SiO_2-Si interface. The tensile mechanical stress value in the ADR therefore decreases, and the gettered oxygen flow from the bulk diminishes. The accumulated oxygen atoms in the ADR are gradually pushed to the SiO_2-Si interface. The growing SiO_2 layer can generate silicon interstitials and at the same time also a reorganization of the end of range interstitials into extended lattice defects takes place.

For annealing at 950 °C, the above mentioned processes occur so fast that separation of them is no longer possible. Even after half a minute annealing, one can already observe the three processes: arsenic segregation, accumulation of oxygen in the ADR, and an increase of the SiO_2 thickness. After 5 minutes of annealing at 950 °C, the processes of oxygen accumulation and growth of the SiO_2 surface layer are almost completed, and only As diffusion takes place during further anneal.

In Sb^+ implanted Si, the processes of Sb segregation and diffusion during thermal annealing occur much slower than for As^+ implanted Si. Also, the oxygen redistribution towards the surface is practically absent. In our opinion this difference is mainly due to different configurations of mechanical fields in the implanted Si crystal.

Our model experiments show that during thermal annealing, implanted ^{18}O diffuses from the depth of ≈300 nm towards the surface and accumulates at the Si-SiO_2 interface region, clearly revealing the oxygen gettering effect [11].

The observed growth of the screening oxide thickness requires about 10^{15} cm^{-2} oxygen atoms. Assuming that all this oxygen comes from the substrate, it has to be gettered from a layer thickness of about 12 µm from the surface assuming a concentration of oxygen in the bulk of 10^{18} cm^{-3}. Taking into account that the gettering time of oxygen from such depth takes about 5 min at 950 °C, the oxygen diffusivity can be estimated to be about 1×10^{-10} cm^2/s. This is about an order of magnitude larger than the typical value reported in literature for bulk Si, which is close to 7×10^{-12} cm^2/s [13].

4.2 Oxide precipitation and dissolution in the ADR If one considers the appearance of concentration peaks in the $^{60}SiO_2^-$ signal as being due to the presence of SiO_2 precipitates in the As-rich region, the variation of the intensities of these peaks as function of the anneal temperature can be explained as follows. It is well-known that the critical radius for the formation of SiO_2 precipitate depends not only on the supersaturation of interstitial oxygen but also on the supersaturation of the intrinsic point point defects, both vacancies and self-interstitials [14]

$$R_{cr} = \frac{2\sigma\Omega}{kTln\frac{C}{C_{eq}}(\frac{V}{V_{eq}})^{\beta}(\frac{I}{I_{eq}})^{-\gamma}}. \quad (1)$$

σ (≈ 0.43 J/m^2 for SiO_2) is the interface energy of the SiO_x precipitate with the Si matrix [15]. Ω (= 2.25×10^{-29} m^3 for SiO_2) is the volume per oxygen atom in the precipitated silicon oxide phase [16], k the Boltzmann constant and T the temperature. C, V, and I are the concentrations of interstitial oxygen, vacancies, and self-interstitials, respectively. C_{eq}, V_{eq}, and I_{eq} are their equilibrium concentrations, respectively [14, 17]. β and γ are the number of vacancies and interstitials, respectively, absorbed in the precipitate per precipitated oxygen atom. Hereby one should take into account that the formation energies of the intrinsic point defects also depend on the Fermi level position and to some extent also to the stress introduced by the large concentration of substitutional dopant atoms and also by the precipitate itself [18, 19].

Equation (1) shows that a vacancy supersaturation leads to enhanced precipitation due to a decrease of the critical radius R_{cr}. The higher vacancy supersaturation at 750 °C due to the lower vacancy solubility V_{eq} combined with the higher supersaturation of oxygen, can explain the higher intensity of the $^{60}SiO_2^-$ signal peak compared to that at 950 °C. Another reason may be a higher rate of activation of implanted As at 950 °C leading to a decrease of the vacancy supersaturation. In addition, the oxygen concentration driven into the region of As redistribution is higher at 750 °C which, together with smaller oxygen

solubility, leads to a higher oxygen supersaturation and an additional decrease of the critical radius for SiO_x precipitate nucleation.

In the considered view, the decrease in the intensity of the $^{60}SiO_2^-$ signal observed after longer annealing times may be attributed to the dissolution of SiO_x precipitates due to energetically more favorable oxidation at a surface SiO_2 layer as well as due to the possible increase of the concentration of self-interstitials produced by oxidation. According to Eq. (1), an increasing self-interstitial concentration leads to an increase of the critical radius for precipitate nucleation. At the initial stage of annealing, after rapid recombination of part of the implantation induced intrinsic point defects, the As atoms are dominantly in metastable interstitial positions, creating a tensile stressed near surface layer, which enhances oxygen gettering from the wafer bulk to the heavily As doped near surface layer during the anneal.

At 750 °C, this process goes on for about 3 to 6 minutes. Longer annealing leads to activation of part of the As atoms whereby they become substitutional and thus remove vacancies, while the other part of the As atoms is accumulated at the SiO_2-Si interface after rapid diffusion of interstitial As atoms. The tensile stress therefore decrease, the enhanced oxygen flow from the bulk is reduced, and oxygen diffuses gradually from the ADR to the Si-SiO_2 interface, increasing the thickness of the surface oxide.

At 950 °C, these processes of restructuring of the surface layer, oxygen gettering from the wafer bulk and oxide film growth occurs over a much shorter time period (< 1 min). Further growth of the oxide surface layer occurs due to absorption of gettered oxygen for a time from 1 to 5 minutes. Further annealing at 950 °C leads to a change in the As distribution profile partly due to interaction of point defects. Oxygen atoms do not participate in these processes any more.

4.3 The impact of implantation induced mechanical stresses After As or Sb implantation, mechanical stresses of both signs are present in the subsurface layer of the Si substrate. During the initial stages of annealing, a part of implanted dopant atoms become substitutional. This leads to an increase of tensile stresses in the subsurface layer. These stresses lead to gettering of oxygen from the bulk of the wafer. In this subsurface area, oxygen can form stable precipitates of a small sizes, as in the presence of tensile stresses, the critical precipitate size is smaller compared to that in the unstrained Si matrix. With increasing annealing time, the situation is completely different for the samples implanted by Sb and As.

While in the case of Sb implantation, the tensile stress is still dominant, in the case of As implantation, a mechanical stress gradient is created as these samples contain both compressively and tensile stressed regions. Perhaps this is due to different mechanisms of diffusion of these impurities in Si. The diffusion of Sb occurs through vacancies, but As atoms diffuses involving silicon self-interstitials [20, 21]. Sb atoms are moving deeper into the wafer consistently occupy vacancies until the full fixing of the atom in the substitutional position. This process is not accompanied by an increase of self-interstitials in the ADR. In contrast to Sb, the As movement into depth and occupation of the substitutional position is accompanied by the release of self-interstitials.This is manifested in the XDS spectra as signal growth from the defects of interstitial type. The increased concentration of self-interstitials in the ADR suppresses oxide precipitate formation and cau ses dissolution of precipitates with subcritical size due to the increase of R_{cr}. Part of the released oxygen diffuses to the surface leading to an increase of the thickness of the screening oxide.

5 Conclusion The impurity distribution profiles and defect formation in near surface layers of Si wafers implanted with 5 keV As or Sb ions have been investigated before and after annealing. It is shown that implantation leads to stresses in the near surface layer, of approximately equal magnitude for both types of ions. Annealing at 750 °C leads to an increase of the tensile stresses in the Sb implanted samples, while in the As implanted samples a mechanical stress gradient is created as these samples contain both compressively and tensile stressed regions. During the initial stages of annealing of As implanted Si, gettering of oxygen in the subsurface layer is observed accompanied by an increasing thickness of the screening oxide, whereas for the Sb implanted Si, this oxygen gettering effect is not observed. It is proposed that the observed oxygen gettering is driven by the mechanical stress gradient which develops during annealing of the As^+ implanted Si samples.

References

[1] International Technology Roadmap for Semiconductors (2012).
[2] D. Kruger, H. Rucker, B. Heinemann, V. Melnik, R. Kurps, and D. Bolze, J. Vac. Sci. Technol. **22**, 455 (2004).
[3] H. Rucker, B. Heinemann, R. Barth, D. Bolze, V. Melnik, R. Kurps, and D. Kruger, Appl. Phys. Lett. **82**, 826 (2003).
[4] H. Shirai, A. Yamaguchi, and F. Shimura, Appl. Phys. Lett. **54**, 1748 (1996).
[5] R. Falster, G.R. Fisher, and G. Ferrero, Appl. Phys. Lett. **59**, 809 (1991).
[6] T. J. Magee, C. Leung, H. Kawayoshi, L. J. Palkuti, B. K. Furman, C. A. Evans, L. A. Christel, J. F. Gibbons, and D. S. Day, Appl. Phys. Lett. **39**, 564 (1981).
[7] I. J. R. Baumvol, F. C. Stedile, S. Rigo, J. J. Ganem, and I. Trimaille, Braz. J. Phys. **24**, 529 (1994).
[8] T. Hirao, G. Fuse, K. Inoue, S Takanayagi, Y. Yaegashi, and S. Ichikawa, J. Appl. Phys. **50**, 5251 (1979).
[9] R. Kögler, E. Wieser, J. Albrecht, and P. Knothe, Phys. Status Solidi A **113**, 321 (1989).
[10] G.-H. Lu, Q. Wang, and F. Liu, Appl. Phys. Lett. **92**, 211906 (2008).
[11] O. Oberemok, V. Kladko, V. Litovchenko, B. Romanyuk, V. Popov, V. Melnik, A. Sarikov, O. Gudymenko, and J. Vanhellemont, Semicond. Sci. Technol. **29**, 055008 (2014).

[12] O. I. Gudymenko, V. P, Kladko, V. P. Melnik, Ya. M. Olikh, V. G. Popov, B. N. Romanyuk, M. V. Slobodian, and P. P. Kogutyuk, Ukr. J. Phys. **53**, 140 (2008).
[13] R. C. Newman, J. Phys.: Condens. Matter **12**, R335 (2000).
[14] J. Vanhellemont and C. Claeys, J. Appl. Phys. **62**, 3960 (1987); J. Appl. Phys. **71**, 1073 (1992).
[15] A. Borghesi, B. Pivac, A. Sassella, and A. Stella, J. Appl. Phys. **77**, 4169 (1995).
[16] V. G. Litovchenko, I. P. Lisovskyy, V. P. Kladko, S. O. Zlobin, M. V. Muravska, A. A. Efremov, and M. V. Slobodyan, Ukr. J. Phys. **5**, 958 (2007).
[17] A. Sarikov, V. Litovchenko, I. Lisovskyy, M. Voitovich, S. Zlobin, V. Kladko, N. Slobodyan, V. Machulin, and C. Claeys, J. Electrochem. Soc. **158**, H772 (2011).
[18] J. Vanhellemont, E. Kamiyama, and K. Sueoka, ECS J. Solid State Sci. Technol. **2**, 166 (2013).
[19] K. Sueoka, E. Kamiyama, and J. Vanhellemont, J. Appl. Phys. **114**, 153510 (2013).
[20] A. Ural, P. B. Griffin, and J. D. Plummer, J. Appl. Phys. **85**, 6440 (1999).
[21] P. M. Fahey, P. B. Griffin, and J. D. Plummer, Rev. Mod. Phys. **68**, 289 (1989).